Genetic remodeling of protein glycosylation *in vivo* induces autoimmune disease

Daniel Chui*†‡, Gayathri Sellakumar*†‡, Ryan S. Green*†, Mark Sutton-Smith§, Tammie McQuistan†, Kurt W. Marek*†, Howard R. Morris§, Anne Dell§, and Jamey D. Marth*†¶

*Glycobiology Research and Training Center, Howard Hughes Medical Institute, †Department of Cellular and Molecular Medicine, University of California at San Diego, La Jolla, CA 92093; and §Department of Biochemistry, Imperial College of Science, Technology and Medicine, London SW7 2AY, England

Edited by Stuart A. Kornfeld, Washington University School of Medicine, St. Louis, MO, and approved December 1, 2000 (received for review August 9, 2000)

Autoimmune diseases are among the most prevalent of afflictions, yet the genetic factors responsible are largely undefined. Protein glycosylation in the Golgi apparatus produces structural variation at the cell surface and contributes to immune self-recognition. Altered protein glycosylation and antibodies that recognize endogenous glycans have been associated with various autoimmune syndromes, with the possibility that such abnormalities may reflect genetic defects in glycan formation. We show that mutation of a single gene, encoding α-mannosidase II, which regulates the hybrid to complex branching pattern of extracellular asparagine (N)-linked oligosaccharide chains (*N*-glycans), results in a systemic autoimmune disease similar to human systemic lupus erythematosus. α-Mannosidase II-deficient autoimmune disease is due to an incomplete overlap of two conjoined pathways in complex-type *N*-glycan production. Lymphocyte development, abundance, and activation parameters are normal; however, serum immunoglobulins are increased and kidney function progressively falters as a disorder consistent with lupus nephritis develops. Autoantibody reactivity and circulating immune complexes are induced, and anti-nuclear antibodies exhibit reactivity toward histone, Sm antigen, and DNA. These findings reveal a genetic cause of autoimmune disease provoked by a defect in the pathway of protein *N*-glycosylation.

autoimmunity | genetics | lupus | glomerulonephritis

Autoimmune diseases afflict an estimated 5% of the human population, yet inherited genetic susceptibilities and causes are for the most part unknown (1, 2). The immune system recognizes glycan-dependent features in self-/non-self-discrimination, and distinct changes in protein glycosylation have been reported in various autoimmune syndromes (3–7). The first autoantibodies to be discovered were the cold agglutinins that bind to glycan chains (termed I/i antigens) and appear to be responsible for approximately 20% of human autoimmune hemolytic anemia cases (3). Elevated levels of autoantibodies to glycolipids are noted in various neurologic disorders, including motor neuron disease (3). Altered glycosylation may also affect immune complex formation. Immunoglobulins with affinity for the Fc region of IgG molecules are found in rheumatoid arthritis, and the severity of the disease is associated with the extent of galactose-deficient *N*-glycans on Fc (8). Human IgA nephropathy has been associated with altered *O*-glycosylation of the IgA1 hinge region and Ig deposition in the kidney (9, 10). Another possible role for aberrant glycan production in autoimmune disease includes Tn syndrome, in which reduced transcription of the core 1 *O*-glycan β1–3 GalT enzyme occurs among hematopoietic compartments. This reduced transcription results in exposure of the Tn antigen on cell surfaces, and some patients suffer hemolytic anemia, thrombopenia, and leukopenia, likely because of the presence of anti-Tn antibodies found in normal serum (11).

Glycan structures can clearly participate in pathogenic processes. Yet determining whether glycan recognition and production abnormalities are a cause of autoimmune disease or are secondary events induced by lesions in other metabolic pathways has awaited studies involving *in vivo* genetic modifications of the glycosylation program itself. Golgi-resident glycosidase and glycosyltransferase enzymes operating in the glycan synthesis pathways are thereby hypothetically promising targets of genetic studies aimed at gaining further insights into the pathogenesis of autoimmune disease.

The α-mannosidase II enzyme is encoded by a single gene in mammals and resides in the Golgi apparatus, where it trims two mannose residues from hybrid N-linked oligosaccharides. This trimming of the mannose residues allows the subsequent addition of multiple glycan branches by glycosyltransferases, as required for the generation of complex *N*-glycans—the most prevalent and diverse forms found on mammalian cell surfaces (12–15). Nonerythroid cells from mice lacking a functional α-mannosidase II gene were unexpectedly found to compensate for this defect by the activity of another α-mannosidase defining an alternative pathway (Fig. 1 and ref. 14). In erythroid cells, glycoproteins were expressed normally at the cell surface, but their portfolio of attached carbohydrate structures was altered with a loss of complex *N*-glycan branching concurrent with an induction of hybrid *N*-glycan forms. These animals exhibit a non-life-threatening dyserythropoiesis similar to human congenital dyserythropoietic anemia type II (14).

We have since observed an increased morbidity of aged mice lacking α-mannosidase II and have therefore attempted to determine whether the loss of α-mannosidase II in some tissues is not fully compensated for by the alternative pathway and leads to physiologic defects among nonerythroid cell types. Our findings herein have revealed that α-mannosidase II is essential for promoting complex *N*-glycan branching to varying degrees in different tissues and cell types and on subsets of glycoproteins. The resulting alteration of *N*-glycan branching provokes a systemic autoimmune disease, indicating that inheritance of an abnormal protein *N*-glycosylation pathway is an etiologic factor in the pathogenesis of autoimmunity.

Materials and Methods

Mice. The null allele for α-mannosidase II (14) was bred into the C57BL/6 genetic background for more than eight generations before these studies. The mice were maintained in a restricted-access barrier facility under specific pathogen-free conditions.

Lectin Blotting. Membrane and total cellular proteins were isolated from various tissues, and complex *N*-glycans were visualized by binding to E-phytohemagglutinin lectin as previously described (14).

Mass Spectrometry. *N*-Glycans were isolated from protein by peptide:*N*-glycanase F (PNGase F) treatment and subjected to various

This paper was submitted directly (Track II) to the PNAS office.

Abbreviations: PFA, paraformaldehyde; PNGase F, peptide:*N*-glycanase F.

‡D.C. and G.S. contributed equally to this work.

¶To whom reprint requests should be addressed at: Howard Hughes Medical Institute, 9500 Gilman Drive-0625, University of California San Diego, La Jolla, CA 92093. E-mail: jmarth@ucsd.edu.

The publication costs of this article were defrayed in part by page charge payment. This article must therefore be hereby marked "*advertisement*" in accordance with 18 U.S.C. §1734 solely to indicate this fact.

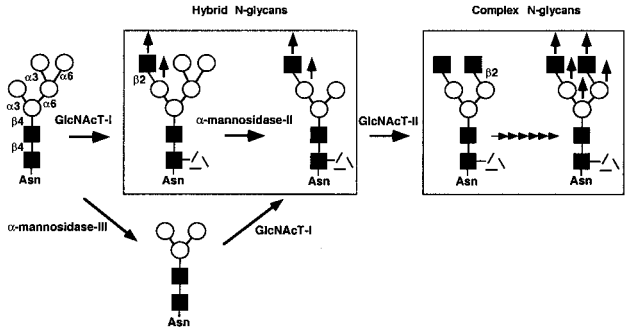

Fig. 1. Two pathways to complex protein *N*-glycosylation in mammals. Complex-type *N*-glycans are produced in the Golgi apparatus and are the predominant forms among extracellular compartments. Each pathway depends on a separate α-mannosidase activity to produce the hybrid *N*-glycan substrate for the GlcNAcT-II glycosyltransferase. Differential use of each pathway among glycoprotein substrates indicates additional controls in *N*-glycan repertoire expression. Black square, *N*-acetylglucosamine; open triangle, fucose; black circles, galactose; open circles, mannose. Anomeric linkage states are denoted. The α1–6 linkage of fucose to the asparagine-proximal *N*-acetylglucosamine (dashed lines) can be found on both hybrid and complex *N*-glycans.

glycosidases before analysis by mass spectrometry, as previously described (16).

Histology. Tissues were fixed in formalin (Fisher Scientific) for 24 h then sequentially dehydrated in increasing ethanol concentrations before they were embedded in paraffin. A microtome (Leica, Deerfield, IL) was used to obtain 3 to 5-μm paraffin sections for staining with hematoxylin and eosin. For immunofluorescence, except for anti-C3, tissues were frozen in Optimal Cutting Temperature medium (VWR Scientific) and sectioned to 3 μm. An ultramicrotome (Leica FCS) was used to obtain 1-μm sections from tissue fixed in 4% paraformaldehyde (PFA) for 1 h, followed by fixation in 8% PFA for 15 min, and cryoprotected in polyvinylpyrrolidone sucrose for analysis with anti-C3 (ICN and Cappel) at 1:50 dilution. An FITC-conjugated anti-goat secondary antibody was used to visualize anti-C3 staining. Frozen samples were fixed with acetone, rinsed with PBS, and incubated in PBS with 10% FCS for 30 min before staining with FITC-conjugated goat anti-mouse antibody specific to IgA, IgM, IgG, IgG1, IgG2a, IgG2b, or IgG3 (Southern Biotechnology Associates) at 1:500 dilution for 60 min at 22°C. Slides were washed in PBS and coverslip mounted for immunofluorescence viewing with a Zeiss Axioplan.

Electron Microscopy. Mouse kidneys were perfused with PBS (20 min) and fixed by 4% PFA for 30 min. The cortex was cut into 1-mm cubes and immersion fixed in 4% PFA (45 min) and 8% PFA (15 min). Tissues were processed, sectioned, labeled with a 10-nm gold-conjugated goat anti-mouse IgG + IgM (H + L), and examined by electron microscopy as described (17).

Urinalysis. Urine was collected from mice and tested with Multistix 10SG (Bayer, Elkhart, IN) reagent strips. Hematuria (trace–large) and proteinuria (trace–2000 mg/dl) were quantified by color. For proteinuria, a positive result was chosen as a minimum value of 100 mg/dl.

Hematology, Flow Cytometry, and Lymphoid Activation. Hematopoietic profiles of mutant mice and littermates were acquired with a CELL-DYN flow cytometer with manual differential counts on glass slides, with the use of Wright–Giemsa, as described (18). Nucleated circulating cells and single-cell suspensions of thymus, spleen, lymph nodes, and bone marrow were collected as described (18). Leukocytes were analyzed with anti-B220-FITC, CD4-FITC, IgM-phycoerythrin, Gr-1-phycoerythrin, Mac-1-FITC (PharMingen), and CD8-Tricolor (Caltag, South San Francisco, CA). Data were analyzed on a FACScan flow cytometer with CELLQUEST software (Becton Dickinson). T and B lymphocytes were purified by a negative sorting strategy following the Dynabead protocol (Dynal, Great Neck, NY). B cells were purified by the use of biotinylated anti-Thy-1.2, CD43 (S7 clone), Ter-119, NK-1.1, Gr-1, and Mac-1 (PharMingen) and streptavidin magnetic beads (Dynal). $CD4^+$ and $CD8^+$ T cells were purified by first removing B cells with Dynal sheep anti-mouse IgG magnetic beads followed by a negative sorting approach that uses biotinylated anti-Gr-1, Ter-119, NK-1.1, and one of either anti-CD4 or CD8 with streptavidin magnetic beads. Lymphoid proliferation was analyzed as described (19,20).

Serum Ig Levels. Serum Ig levels were measured as previously described (19).

Anti-nuclear Antibodies. For anti-nuclear antibody detection, mice sera were diluted to 1:250 in PBS and incubated with HEp-2 cell substrate slides (Immuno Concepts, Sacramento, CA) in a covered humidified chamber for 30 min at 22°C. Slides were rinsed in PBS for 20 min, and antibody was detected with the use of FITC-conjugated anti-mouse IgG + IgM (Jackson ImmunoResearch) at 1:250 for 30 min at 22°C. Slides were washed in PBS and mounted with coverslips for viewing. Plates coated with indicated antigens and C1q to detect circulating immune complexes (CIC) (Alpha Diagnostic International, San Antonio, TX) were used with sera diluted by 1:400 in the buffers supplied.

Autoantibody Characterization. Tissue homogenates were produced in lysis buffer (5% 1 M Tris·HCl, pH 7.5/3% 5 M NaCl/1% Triton X-100 detergent) with the use of Kontes–Duall tissue grinders (Fisher) and coated at 10 μg/ml for 1 h at 37°C into 96-well Nunc Maxisorp plates (Fisher). Plates were washed three times with 150 μl PBS with 0.05% Nonidet P-40 and incubated with 2% BSA in PBS for 1 h at 37°C. Plates were washed, and serial dilutions of wild-type and mutant sera (in PBS with 1% BSA) were added for 90 min at 37°C. Plates were washed and incubated with 100 μl of an alkaline phosphatase-conjugated anti-mouse Ig κ light-chain monoclonal antibody (PharMingen) in PBS with 1% BSA at 1:5000 for 45 min at 22°C. Plates were washed and developed with 100 μl of *p*-nitrophenyl phosphate (Sigma) for 15 min at 22°C, and reactions were stopped with 50 μl of 0.1 M EDTA. Plates were read on a VERSAmax microplate reader at 405 nm (Molecular Devices). Removal of *N*-glycans was accomplished by boiling 100 μg of homogenate for 3 min in buffer containing 50 mM sodium phosphate (pH 7.5 generated with NaH_2PO_4 and Na_2HPO_4), 0.4% SDS, and 8% 2-mercaptoethanol before the addition of 5 milliunits of PNGase F (Calbiochem) in 1% Nonidet P-40 and 2% sodium phosphate (pH 7.5). This procedure was followed by a 24-h incubation at 37°C. Tissue homogenates (20 μg) were subjected to SDS/PAGE, transferred to nitrocellulose, and incubated with 5% BSA in TBS (20 mM Tris·HCl, pH 8.0/150 mM NaCl) for 2 h. Blots were then incubated with sera (1:2000 dilution) in TBS with 1% BSA, or with biotinylated Con A (Sigma) at 50 ng/ml in TBS with 0.1 mM $MgCl_2$, 0.1 mM $MnCl_2$, 0.1 mM $CaCl_2$, 0.05% Nonidet P-40, and 1% BSA for 90 min at 22°C. Autoantibody binding was detected with the use of enhanced chemiluminescence (Amersham Pharmacia) after a 45-min incubation with a horseradish peroxidase-conjugated anti-κ light chain monoclonal antibody (PharMingen) at 1:10,000 in TBS with 0.05% Nonidet P-40. Con A binding was detected with enhanced chemiluminescence after a 45-min incubation with horseradish peroxidase-conjugated streptavidin (Vector Laboratories) at 1:10,000 in TBS with 0.05% Nonidet P-40 and an overnight wash.

Results

The degree to which the alternative α-mannosidase pathway compensates for the absence of α-mannosidase II in various

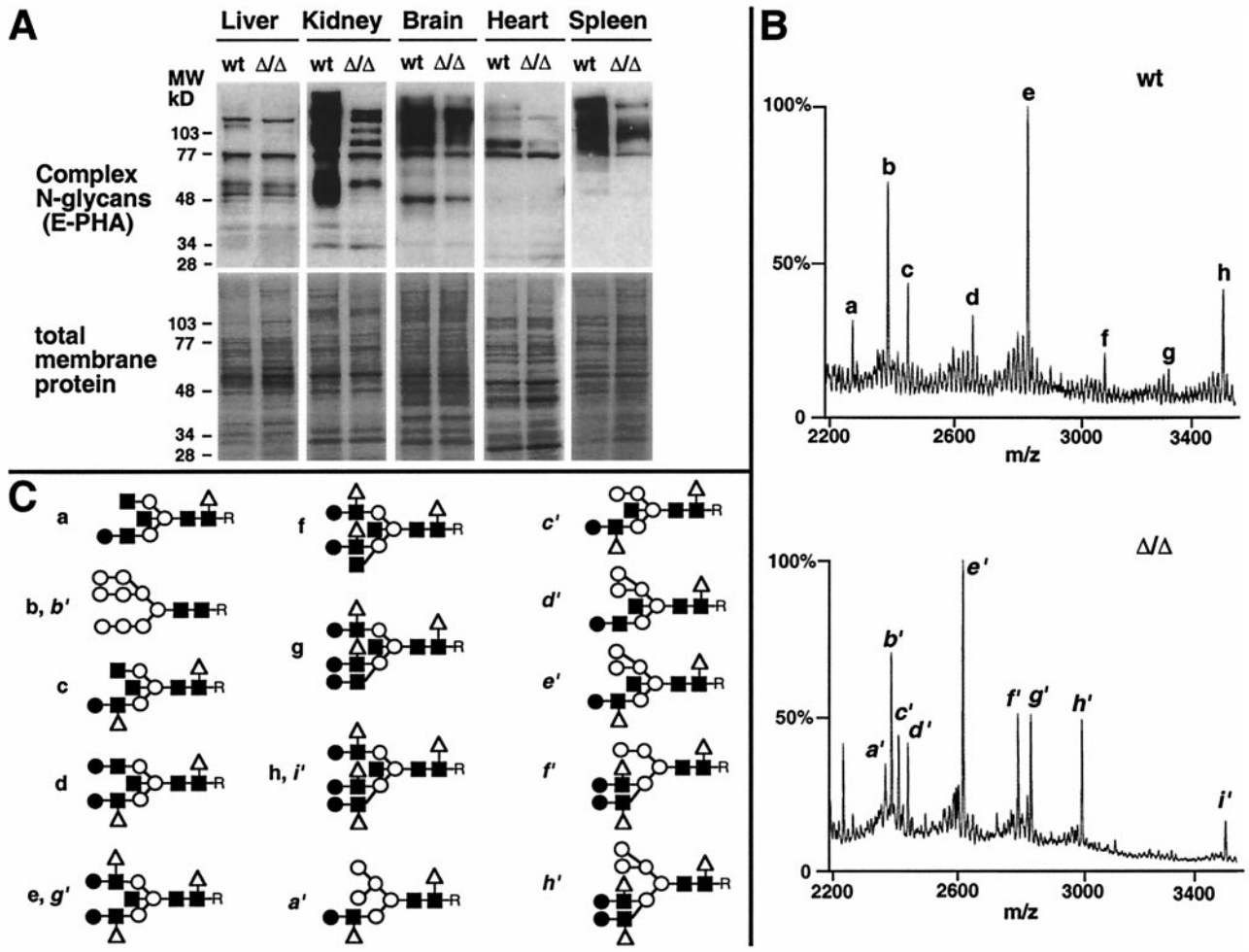

Fig. 2. Reduction in complex *N*-glycans and increased hybrid *N*-glycan structures in the absence of α-mannosidase II. (*A*) Complex *N*-glycans are deficient on glycoproteins from some tissues in mice homozygous for a deletion in the α-mannosidase II gene (Δ/Δ). Membrane protein was isolated from various tissues, and complex *N*-glycans were visualized by binding to E-phytohemagglutinin (*Upper*) as previously described (14). Equivalent amounts of membrane protein were used in the analyses (*Lower*). (*B*) Mass spectrometry of *N*-glycans from various tissues (kidney shown) was accomplished after isolation from glycoproteins by PNGase F. Subsequent treatment with various glycosidases (not shown) provided additional information on specific saccharide linkages (16). (*C*) *N*-Glycan structures (desialylated) defined by mass spectrometry from wild-type tissues were mostly complex types with fully modified mannose termini bearing *N*-acetylglucosamine linkages (*a, c–h*), whereas structures in the absence of α-mannosidase II contained hybrid *N*-glycans noted by terminal mannose residues (*a′*, *c′*, *d′*, *e′*, *f′*, *h′*). The anomeric glycosidic linkages among the core regions are indicated (Fig. 1). Antennary extensions are with β1–2-linked glucosamine, β1–4-linked galactose, and α1–6-linked fucose and are as described for the relevant Lewis antigens (38). R indicates the position of the asparagine residue before release of *N*-glycans from glycoproteins by PNGase F. For monosaccharide symbols, see Fig. 1 legend.

tissues was investigated. With the use of the E-phytohemagglutinin lectin as a probe for complex *N*-glycans, we analyzed glycoproteins derived from various organs of α-mannosidase II-deficient mice (see *Materials and Methods*). Some glycoproteins appeared to be quantitatively affected and exhibit reduced levels of complex *N*-glycans, whereas a few appeared fully dependent on α-mannosidase II for hybrid to complex-type *N*-glycan synthesis (Fig. 2*A*). The glycosylation of kidney glycoproteins with complex *N*-glycans is especially dependent on α-mannosidase II. In contrast, various glycoproteins in different tissues did not appear to require α-mannosidase II as they retained normal E-phytohemagglutinin binding, indicating that the alternative pathway is sufficient for them to be modified appropriately with complex *N*-glycans.

With the use of recently developed mass spectrometry approaches for determining glycan structures in mammalian tissue (16), we defined the specific *N*-glycan branch structures expressed in tissues of wild-type and α-mannosidase II-deficient mice. These studies revealed a significant reduction of known complex *N*-glycans along with the induction of specific hybrid *N*-glycan structures in mice lacking α-mannosidase II (Fig. 2 *B* and *C*). Hybrid *N*-glycans are not prevalent in normal adult tissues, and two of the structures elucidated in the absence of α-mannosidase II are biantennary Lewis X hybrid *N*-glycan sequences not previously identified in any mammalian source (Fig. 2*C*, *f′* and *h′*). These data together indicate that α-mannosidase II function is varied among nonerythroid cell types by mechanisms that may involve restricted substrate access or perhaps distinct glycoprotein substrate preferences of GlcNAcT-I and α-mannosidase III. We inferred that α-mannosidase II may be uniquely essential for specific physiologic processes involving nonerythroid cells, which prompted us to closely investigate the physiology of aging α-mannosidase II-deficient mice.

A small but significant increase in mortality by 18 months of age was noted specifically among mice lacking α-mannosidase II. On histological examination of multiple organs, glomerulonephritis was detected in over 80% of more than two dozen

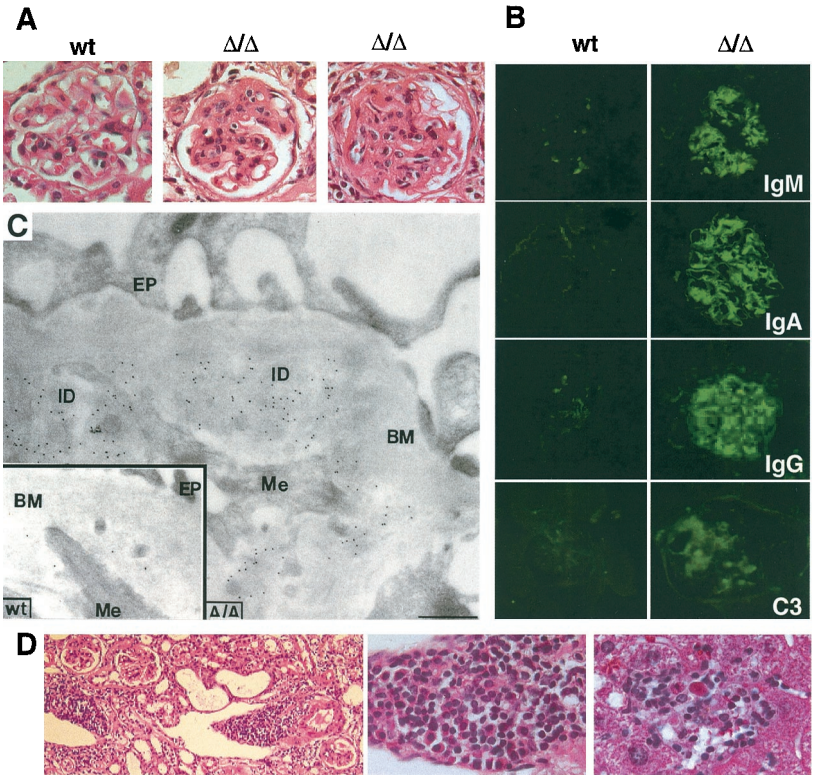

Fig. 3. Immune complex glomerulonephritis in the absence of α-mannosidase II. (*A*) In comparison with glomeruli from wild-type mice (*Left*), thickening of the mesangium is observed with capillary lumen obstruction in mutant mice (*Center* and *Right*). (Hematoxylin/eosin stain of glomeruli at ×100 magnification is shown.) (*B*) The glomeruli of mice lacking α-mannosidase II contain high levels of Ig deposits composed of IgM, IgA, and IgG [the latter include IgG1, IgG2a, and IgG2b (not shown)], as well as complement component C3 (×400 magnification shown). Antibody deposits were also noted in other tissues, including lung and liver, but to a lesser extent (not shown). (*C*) Immunogold labeling of a glomerulus from a mutant mouse, showing immune deposits (ID) between the glomerular basement membrane (BM) and mesangial cell processes (Me). Gold particles indicate the presence of IgG/IgM in the ID. (*Inset*) Similar field from a wild-type mouse, showing few gold particles. EP, Foot processes of glomerular epithelium (bar, 0.5 μm). (*D*) Mononuclear leukocytic infiltrates in kidney (*Left* and *Center*) and liver of mutant mice (×400): lymphocytes, plasma cells, and neutrophils. Infiltrates in liver (*Right*) are found with evidence of hepatocyte degeneration and accumulated bile. Results shown are from mice that are either 8 months (*A, B,* and *D*) or 13 months (*C*) of age.

12-month-old mutant animals surveyed, whereas wild-type kidneys were unaffected. We noted extensive scarring of the kidneys in the majority of mutant animals more than 12 months old, and the increased mortality correlated with necrotic and sometimes cystic kidneys (data not shown). By 12 months of age, glomeruli exhibited an expanded mesangial matrix to the extent that the lumen of capillaries was often obstructed (Fig. 3*A*). Before disease onset and by 3 months of age, ≈50% of mutant animals contained elevated Ig deposition in kidney glomeruli, and by 6 months of age >80% showed heavy Ig depositions that included IgM, IgA, and IgG (Fig. 3*B*). In addition, complement component C3 deposition was also elevated (Fig. 3*B*). Electron microscopic analysis revealed that antibody deposition occurred specifically in the extended mesangial matrix and not at the glomerular basement membrane, whereas increased numbers of mesangial cell nuclei were also observed (Fig. 3*C* and data not shown). Mononuclear leukocytic infiltrates were also frequently elevated in kidney, liver, and lung tissue of mutant mice. These infiltrates were composed primarily of lymphocytes but included plasma cells and some neutrophils (Fig. 3*D* and data not shown).

These pathohistological findings suggest lupus nephritis involving renal antigens or the trapping of circulating immune complexes during glomerular filtration (21, 22). Although the identification and pathogenic role of self-antigens in immune complexes are mostly unresolved (23, 24), immune complex deposition can cause glomerular damage. In some circumstances this damage depends on the presence of the γ chain of the Fc receptor (25). Even in the absence of complement and Fc involvement, Ig deposition at the glomerular basement membrane can cause glomerular damage with increased permeability leading to proteinuria and hematuria (26, 27). Unlike membranous nephritis in which antibody binding to the glomerular basement membrane is diagnostic and is associated with moderate to severe proteinuria, only 30% of α-mannosidase II-deficient mice exhibited proteinuria, and this condition was a low to moderate type, whereas 60% exhibited moderate hematuria. Before 3 months of age, the kidneys functioned normally in all mutant mice, with no evidence of abnormalities by urinalysis or by serum chemistry analyses of renal function (data not shown).

Autoimmune disease may result from immune cell-intrinsic defects that can be detected in assays of lymphoid development and function. We noted that beginning by 10 weeks of age, serum levels of IgM, IgA, and IgG were elevated in mice lacking α-mannosidase II (Fig. 4*A*). Nevertheless, B and T lymphocyte development, abundance, and function appeared normal. With the exception of the spleen in which increased levels of nucleated erythroid precursors are found (14), we observed normal cellularity in lymphoid organs and no evidence of leukocytosis in any compartment (Fig. 4*B*). Normal frequencies of $CD4^+$ and $CD8^+$ T cells and $B220^+$ B cells were observed, and peripheral T lymphocytes expressed a normal Vα and Vβ T cell receptor repertoire (Fig. 4*B* and data not shown). With increasing age and in mice with kidney disease as detected by urinalysis, approximately 25% of animals exhibited an elevated level of memory T cells ($CD44^+Ly6C^+CD4^+$ and $CD44^+Ly6C^+CD8^+$) among slightly to moderately enlarged lymph nodes (data not shown). However, the $CD5^+$ peritoneal B-1 lymphocyte population levels were seldom elevated. Other cell surface glycoproteins associated with T and B lymphocyte activation, including B7, CD23, IL-2 receptor and molecules comprising the major histocompatibility complex, were expressed at levels that are normal for mature naive lymphocytes, and antibody glycosylation itself was not affected by lectin analysis (data not shown). In addition, T and B lymphocyte proliferation responses to antigen receptor crosslinking were found to be within normal response parameters (Fig. 4*C*). These immunological findings do not reflect the lymphoid hyperactivity and dysfunction observed in other rodent models of autoimmune disease.

A systemic autoimmune disease was indicated on further immunological analyses of α-mannosidase II-deficient mice. At any one time, more than 60% of α-mannosidase II-deficient mice with hematuria exhibited anti-nuclear antibody reactivity toward nucle-

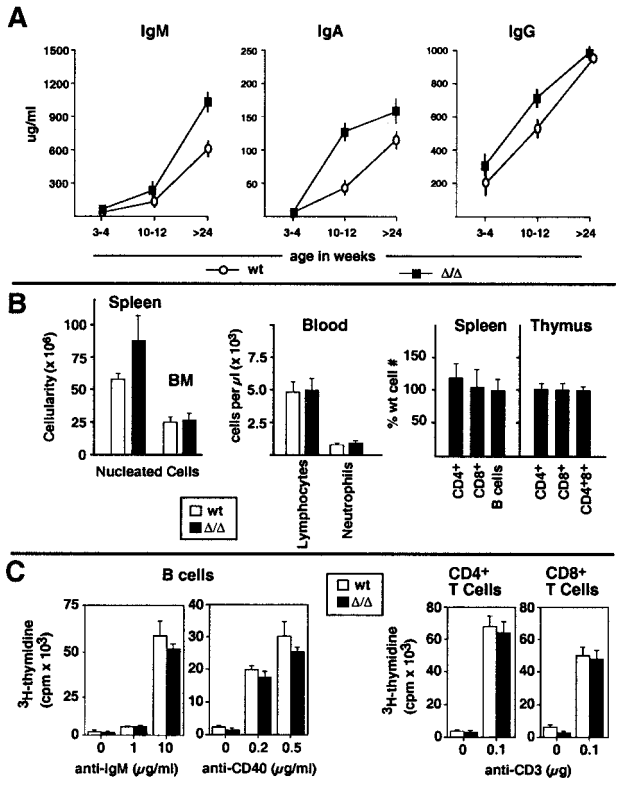

Fig. 4. Hematopoietic and immune parameters in the absence of α-mannosidase II. (*A*) Serum Ig levels comprising IgM, IgA, and IgG were elevated by 10 weeks of age (16 mice of each genotype used). Elevations in IgG levels included IgG1, IgG2a, and IgG2b, whereas no changes were seen in IgE or IgG3 levels (not shown). (*B*) Lymphocyte cellularity was not altered among lymphoid organs or in circulation. Increased cellularity in the spleen was due to increased numbers of nucleated erythroblasts, as described (14). Frequencies of T cells ($CD4^+$ and $CD8^+$) and B cells ($B220^+$) were also normal. (*C*) T and B cell proliferation after antigen receptor crosslinking was unaffected. At east five mice of each genotype were studied.

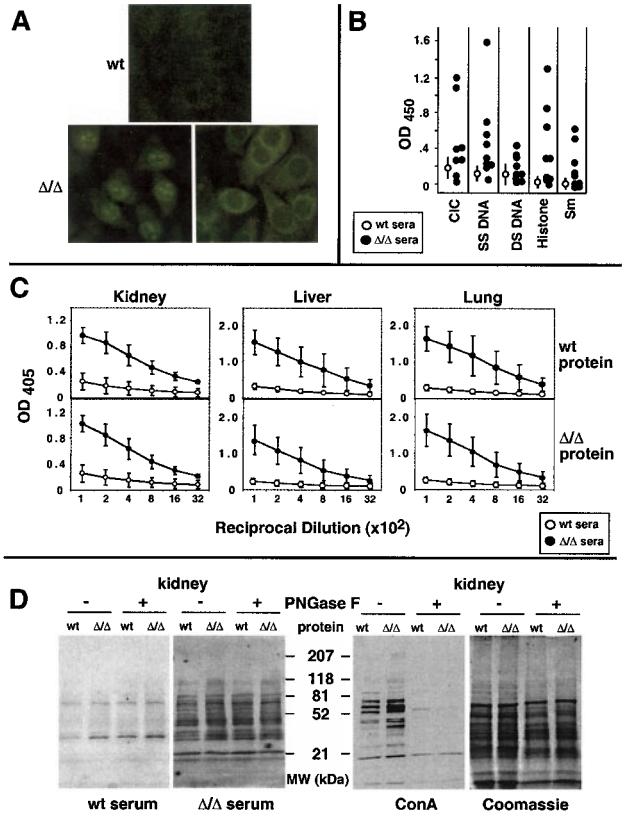

Fig. 5. Anti-nuclear antibodies and autoantibodies are found in mice lacking α-mannosidase II. (*A*) Reactivity of wild-type sera (wt) or α-mannosidase II deficient sera (Δ/Δ) to HEpG2 cells visualized by fluorescent microscopy (×200). Nucleolar (*Bottom left*) and nuclear membrane (*Bottom right*) binding by immunoglobulins in the sera of different mice. Sera dilutions were 1:250. (*B*) Autoantibody reactivity to various nuclear antigens. Eight mice of each genotype were tested (wild type plotted as OD ± SD, Δ/Δ plotted individually). (*C*) Autoantibodies to kidney, lung, and liver proteins are induced in α-mannosidase II-deficient mice. Similarly increased autoreactivity is noted when wild-type protein or α-mannosidase II-deficient protein is used as the substrate. (*D*) Cellular proteins of the indicated genotype were subjected to SDS-PAGE with or without PNGase F pretreatment. Protein blots were incubated with indicated sera (1:2,000 dilution) and processed as described (*Materials and Methods*). Identical genotypes represent autologous samples in *C* and *D*.

olar as well as nuclear envelope epitopes (Fig. 5*A*). Antibodies that bound histone, Sm antigen, double-stranded DNA, and single-stranded DNA were also detected (Fig. 5*B*). In addition, circulating immune complexes were frequently elevated, indicating that some fraction of the immune deposition in the kidney may reflect immune complex trapping. Autoantibodies to autologous protein from the kidney, liver, and lung were also elevated (Fig. 5*C*). The increased titers of autoantibody reactivity were not significantly affected by the removal of *N*-glycans from denatured protein with the use of PNGase F (Fig. 5*D*). Although *N*-glycan-dependent reactivity to native *N*-glycosylated glycoprotein conformations cannot be determined, our findings suggest that most autoantibody is produced against a wide range of intracellular and nuclear proteins induced, perhaps by increased phagocytosis and self-antigen presentation that commonly appears in systemic autoimmune disease (2). Taken together with the above spectrum of phenotypic findings, our results reveal a systemic autoimmune disease that is remarkably similar to human systemic lupus erythematosus.

Discussion

Currently identified causes of autoimmune disease encompass modifications of lymphocyte activation or development, chemical or pathogenic exposure, and changes in histocompatibility complex expression (1, 28, 29). We have found that an autosomal recessive genetic defect in the pathway of protein *N*-glycosylation is also a unique factor capable of inducing systemic autoimmune disease exhibiting symptoms found in human systemic lupus erythematosus, including hematological disorder, immunological disorder (anti-DNA or anti-Sm), renal disorder, and anti-nuclear antibody (30). Examples of single gene lesions that provoke systemic autoimmune disease involve SHP-1, CD22, CTLA-4, IL-2, IL-4, PD-1, transforming growth factor-β, Fas, Fas ligand, the T cell antigen receptor, and the *lyn* tyrosine kinase. These defects overtly alter lymphocyte development, abundance, viability, or immune responses (2). The emergence of systemic autoimmune disease can also reflect the involvement of multiple genes. For example, the NZB and NZB/NZW F_1 autoimmune mouse models result from defects in multiple genes and exhibit B lymphocyte immune hyperactivity.

α-Mannosidase II deficiency does not similarly alter lymphoid development, abundance, or proliferation in response to antigen receptor activation and thus is more similar to human systemic autoimmune diseases that also occur without such developmental and immune response abnormalities (2). Although the immune system is obviously the source of increased self-reactivity and thereby involved in the disease process, we have shown that lymphocytes lacking α-mannosidase II continue to produce complex *N*-glycans at the cell surface and at close to normal

levels (14). Our findings support the view that the lymphoid population exists without cell-intrinsic defects that easily explain the origin of this systemic autoimmune disease. Additional studies by adoptive transfer, conditional mutagenesis, and transplantation approaches can further address this possibility.

Although histocompatibility molecules were expressed normally in mice lacking α-mannosidase II, autoimmune disease emergence and severity can be modulated by major histocompatibility haplotypes in some animal models (2). We do not yet know whether MHC haplotype or *N*-glycosylation plays a role in disease etiology. When *N*-glycosylation of MHC is completely abrogated by tunicamycin or by mutagenesis of asparagine residues, unglycosylated MHC infrequently reaches the cell surface, being retained in the endoplasmic reticulum; however, those that are found on the cell surface appear to function normally (31).

Several hundred Golgi-resident glycosidase and glycosyltransferase enzymes orchestrate the repertoire of cell surface glycan structures. Growth and differentiation signals provided during normal and pathologic metabolism regulate the expression of these enzymes (32). The changing enzyme expression levels in the Golgi of a given cell can alter glycan structures present on the cell surface. Nutritional modifications in humans have also been found to influence the extracellular *N*-glycan repertoire (33, 34). Interestingly, ingestion of the α-mannosidase II inhibitor Swainsonine has been reported to alleviate tumor-induced immune suppression, to increase the propensity for lymphocyte activation, and to inhibit tumor growth and metastasis (35). Whether a clinical regime of α-mannosidase II inhibitors can lead to autoimmune disease is not known.

Autoimmunity has been divided into systemic and organ-specific types with common mechanistic underpinnings indicated (36). Systemic autoimmunity can lead to organ-specific disease (37), whereas molecular mimicry, histocompatibility haplotypes, and lymphoid involvement may be crucial for the emergence and progression of both disease types. However, antigens that evoke systemic autoimmune disease and factors influencing disease progression are not well understood (2, 24). The previous association of autoimmune syndromes with the induction of anti-carbohydrate antibodies and with carbohydrate structure abnormalities indicated the possibility that glycan recognition or structural alterations might be pathogenic in some circumstances. We can conclude that it is the altered *N*-glycosylation of one or more glycoproteins that is the cause of systemic autoimmune disease with symptoms of lupus nephritis in the absence of α-mannosidase II.

It is possible that alterations in *N*-glycan branching among some glycoproteins and tissues may result in the formation of unusual epitopes that do not fully participate in the immune determination of self. We find that the alternative pathway in complex *N*-glycan production fails to sufficiently overlap with α-mannosidase II function and results in the production of unusual and sometimes unique hybrid glycan *N*-glycan branches among a subset of glycoproteins and cell types. It is also possible that this abnormal *N*-glycan expression varies in an age-dependent manner by a developmental change in glycoprotein substrate production and the efficacy of the alternative pathway in complex *N*-glycan formation. By whatever means, the loss of α-mannosidase II alters *N*-glycan branching and clearly attenuates the immune system's ability to maintain self-tolerance. It is further intriguing to consider whether α-mannosidase II inhibition bestows its antitumorigenic effect by modulating the immune–autoimmune threshold.

We thank our colleagues, including Larry Goldstein and Ajit Varki, for helpful comments, Marilyn Farquhar for electron microscopic analyses, and Nissi Varki for histological studies. This research was supported by a grant from the Institute of Diabetes and Digestive and Kidney Diseases, National Institutes of Health (DK48247) to J.D.M., grants from the Biotechnology and Biological Sciences Research Council and the Wellcome Trust to H.R.M. and A.D., and a Medical Research Council studentship to M.S.-S. J.D.M. acknowledges support as an Investigator of the Howard Hughes Medical Institute.

1. Steinman, L. (1995) *Cell* **80,** 7–10.
2. Cohen, P. L. (1999) in *Fundamental Immunology*, ed. Paul, W. E. (Lippincott, Philadelphia), pp. 1067–1088.
3. Gleeson, P. A. (1994) *Biochim. Biophys. Acta* **1197,** 237–255.
4. Delves, P. J. (1998) *Autoimmunity* **27,** 239–253.
5. Nyame, A. K., Debose-Boyd, R., Long, T. D., Tsang, V. C. W. & Cummings, R. D. (1998) *Glycobiology* **8,** 615–624.
6. Dighiero, G. & Rose, N. R. (1999) *Immunol. Today* **20,** 423–428.
7. Shamshiev, A., Donda, A., Carena, I., Mori, L., Kappo, L. & De Libero, G. (1999) *Eur. J. Immunol.* **29,** 1667–1675.
8. Parekh, D. B., Dwek, R. A., Sutton, B. J., Fernandes, D. L., Leung, A., Stanworth, D., Rademacher, T. W., Mizuochi, T., Taniguchi, T., Matsuta, K., *et al.* (1985) *Nature (London)* **316,** 452–457.
9. Baharaki, D., Dueymes, M., Perrichot, R., Basset, C., Le Corre, R., Cledes, J. & Youinou, P. (1996) *Glycoconj. J.* **13,** 505–511.
10. Hiki, Y., Kokubo, T., Iwase, H., Masaki, Y., Sano, T., Tanaka, A., Toma, K., Hotta, K. & Kobayashi, Y. (1999) *J. Am. Soc. Nephrol.* **10,** 760–769.
11. Berger, E. (1999) *Biochim. Biophys. Acta* **1455,** 255–268.
12. Kornfeld, R. & Kornfeld, S. (1985) *Annu. Rev. Biochem.* **54,** 631–664.
13. Moremen, K. W., Trimble, R. B. & Herscovics, A. (1994) *Glycobiology* **4,** 113–125.
14. Chui, D., Oh-eda, M., Liao, Y. F., Panneerselvam, K., Lal, A., Marek, K. W., Freeze, H. H., Moremen, K. W., Fukuda, M. N. & Marth, J. D. (1997) *Cell* **90,** 157–167.
15. Schachter, H. (1991) *Glycobiology* **1,** 453–461.
16. Sutton-Smith, M., Morris, H. R. & Dell, A. (2000) *Tetrahedron Asymmetry* **11,** 363–369.
17. Kurihara, H., Anderson, J. A. & Farquhar, M. G. (1995) *Am. J. Physiol.* **268,** F514–F524.
18. Ellies, L. G., Tsubooi, S., Petryniak, B., Lowe, J. B., Fukuda, M. & Marth, J. D. (1998) *Immunity* **9,** 881–890.
19. Hennet, T., Chui, D., Paulson, J. C. & Marth, J. D. (1998) *Proc. Natl. Acad. Sci. USA* **95,** 4504–4509.
20. Priatel, J. J., Sarkar, M., Schachter, H. & Marth, J. D. (1997) *Glycobiology* **7,** 45–56.
21. McCluskey, R. T., Collins, A. B. & Niles, J. L. (1995) in *Diagnostic Immunopathology*, eds. Colvin, R. B., Bhan, A. K. & McCluskey, R. T. (Raven, New York), pp. 109–121.
22. Couser, W. G. (1993) *Kidney Int.* **44,** S19–S26.
23. Tan, E. M. (1991) *Cell* **67,** 841–842.
24. Kotzin, B. L. (1996) *Cell* **85,** 303–306.
25. Clynes, R., Dumitru, C. & Ravetch, J. V. (1998) *Science* **279,** 1052–1054.
26. Salant, D. J., Madaio, M. P., Adler, S., Stilman, M. M. & Couser, W. G. (1981) *Kidney Int.* **21,** 36–43.
27. Couser, W. G., Darby, C., Salant, D. J., Adler, S., Stilman, M. M. & Lowenstein, L. M. (1985) *Am. J. Physiol.* **249,** F241–F250.
28. Nishimura, H., Nose, M., Hiai, H., Miknato, N. & Honjo, T. (1999) *Immunity* **11**, 141–151.
29. Cornall, R. J., Cyster, J. G., Hibbs, M. L., Dunn, A. R., Otipoby, K. L., Clark, E. A. & Goodnow, C. C. (1998) *Immunity* **8,** 497–508.
30. Nakamura, R. M. (1996) in *Clinical Diagnosis and Management*, ed. Henry, J. B. (Saunders, Philadelphia), pp. 1013–1024.
31. Miyazaki, J., Appella, E., Zhao, H., Forman, J. & Ozato, K. (1986) *J. Exp. Med.* **163,** 856–871.
32. Lowe, J. B. & Varki, A. (1999) in *Essentials of Glycobiology*, eds. Varki, A., Cummings, R., Esko, J., Freeze, H., Hart, G. & Marth, J. (Cold Spring Harbor Lab. Press, Plainview, NY), pp. 253–266.
33. Niehues, R., Hasilik, M., Alton, G., Korner, C., Schiebe-Sukumar, M., Koch, H. G., Zimmer, K. P., Wu, R., Harms, E., Reiter, K., *et al.* (1998) *J. Clin. Invest.* **101,** 1414–1420.
34. Marquardt, T., Luhn, K., Srikrishna, G., Freeze, H. H., Harms, E. & Vestweber, D. (1999) *Blood* **94,** 3976–3985.
35. Goss, P. E., Reid, C. L., Bailey, D. & Dennis, J. W. (1997) *Clin. Cancer Res.* **7,** 1077–1086.
36. Shevach, E. M. (1999) in *Fundamental Immunology*, ed. Paul, W. E. (Lippincott, Philadelphia), pp. 1089–1125.
37. Kouskoff, V., Korganow, A.-S., Duchatelle, V., Degott, C., Benoist, C. & Mathis, D. (1996) *Cell* **87,** 811–822.
38. Lowe, J. B. & Marth, J. D. (1999) in *Essentials of Glycobiology*, eds. Varki, A., Cummings, R., Esko, J., Freeze, H., Hart, G. & Marth, J. (Cold Spring Harbor Lab. Press, Plainview, NY), pp. 211–252.